

AUTOCLAVED AERATED CONCRETE WASTE AS A MICRO-FILLER FOR PORTLAND CEMENT

RIMVYDAS KAMINSKAS *, IRMANTAS BARAUSKAS

Faculty of Chemical Technology, Kaunas University of Technology, Radvilenu str. 19, LT-50254, Kaunas, Lithuania

The study aims at investigating the possibility of using Autoclaved Aerated Concrete Waste (AACW) as an additive (replacement) for Portland cement. 5%, 10% and 15% (by weight) of Portland cement were replaced with this additive. The specimens of cement paste were hardened for 28 days under normal conditions in water. It was estimated that recycling of AACW as the micro-filler required one and a half less energy than a natural additive of limestone and four times less energy than conventional construction and demolition wastes i.e. cement mortar. Under normal conditions, Autoclaved Aerated Concrete Waste additive accelerates the initial hydration of ordinary Portland cement (OPC), promotes the formation of additional calcium silicate hydrates, and increases the density of cement stone. It was estimated that up to 10 % wt. of the OPC can be replaced by AACW additive without impairing the strength properties of cement paste samples.

Keywords: Portland cement, Autoclaved Aerated Concrete Waste, additives, energy consumption.

1. Introduction

Fine additives used in cement systems are classified into reactive and “inert” materials [1]. “Inert” additives (quartz, limestone or dolomite) under normal processing conditions fill up the void spaces remaining between the coarser particles and contribute to an increase of compressive strength without any chemical reaction [1, 2]. The reactive additives (i.e., pozzolana, ground blast furnace slag) also fill the void spaces between the larger particles, which is otherwise occupied by water, and, in contrast to “inert” additives, with time they react chemically to produce additional hydrates.

Pozzolans play an important role when are added to Portland cement because they usually increase the mechanical strength and durability of concrete structures. The most important effects in the cementitious paste microstructure are changes in pore structure produced by the reduction in the grain size caused by the pozzolanic effect (PE) and the obstruction of pores and voids by the physical action of the finer grains (filler effect). The pozzolanic and physical effects are maximized with increasing the duration of hydration. When the results for the same strength values are compared, the filler effect (FE) increased more than the pozzolanic effect [3]. Some researchers performed tests with non-pozzolanic fillers [4, 5] to quantify their effect on the increase of concrete strength. Goldman and Bentur [6] studied the effect of the addition of carbon black as a micro-filler, and compared it to the effect of the addition of silica fume on the performance of high-strength concrete. It was found that the mechanism by which silica fume affects the concrete behaviour is of a physical

origin and is based on a micro-filler effect, prior to its action as a pozzolanic material. The micro-filler effect is of greater significance to strength enhancement.

Autoclaved aerated concrete (AAC) is a lightweight microporous building material. Quartz sand (ordinarily – ground sand), gypsum, lime and/or cement and water are used as main components. Aluminium powder is used as a forming gas agent. Aluminium powder reacts with calcium hydroxide and water to form *hydrogen*. The hydrogen gas foams and expands the volume of the raw mix. After gaining initial strength, the concrete array is placed in an *autoclave* chamber. During this steam pressure hardening process, fine quartz sand reacts with *calcium hydroxide* to form *calcium silicate hydrates*, which give AAC its strength and other properties.

Autoclaved Aerated Concrete Waste (AACW) is Autoclaved Aerated Concrete rejected by the manufacturing process. Recycled AACW can be partially used in the production of new AAC yet the amount is limited because of quality issues [7]. As a result, some factories simply send it to the waste dump. On the other hand, such AAC has a lower compressive strength than other affiliated or similar materials in construction and demolition waste (C&D W) and, therefore, it is not suitable for traditional recycling applications [7]. Crushed AAC waste can be also used as oil absorbent or as low-cost filler in the rubber industry [8, 9].

A number of questions regarding Autoclaved Aerated Concrete Waste (AACW) as a micro-filler remain to be addressed. Although there are many studies, the researches concerning the influence of non-pozzolanic micro-filler, which contains a noticeable amount of calcium silicate hydrates, on

* Autor corespondent/Corresponding author,
E-mail: Rimvydas.Kaminskas@ktu.lt

hydration and hardening of Portland cement remains limited. The aim of this investigation was to evaluate the possibility of using Autoclaved Aerated Concrete Waste (AACW) as a micro-filler and to investigate its influence on the hydration and hardening of Portland cement.

2. Materials and Methods

The experiments were performed with treated Autoclaved Aerated Concrete Waste (AACW): it was shattered, dried at 80 °C for 24 h, and ground using a vibrating disc mill to a specific surface area of 450 m²/kg.

The ordinary Portland cement (OPC) CEM I 42.5 R was used in this work. The chemical composition of the cement is shown in Table 1. The mineralogical composition of the OPC is as follows: 3CaO·SiO₂ - 52.97 wt.%; 2CaO·SiO₂ - 19.61 wt.%; 3CaO·Al₂O₃ - 9.16 wt.%; 4CaO·Al₂O₃·Fe₂O₃ - 9.74 wt.%; CaSO₄·2H₂O - 5.37 wt.%.

Table 1

Chemical composition of Portland cement	
Component	wt. %
SiO ₂	19.52
Al ₂ O ₃	5.03
Fe ₂ O ₃	3.05
CaO	61.39
MgO	3.93
K ₂ O	1.06
Na ₂ O	0.12
SO ₃	2.5
Specific surface area, m ² /kg	350

The construction and demolition waste (C&D W) was prepared from hardened cement mortar without a coarse aggregate. The cement paste samples for compressive strength and instrumental analysis (30 × 30 × 30 mm) were formed of ordinary Portland cement (OPC) and Portland cement with 5%, 10%, and 15% AACW replacement. The ratio of water to cement was 0.3. During the first day, the samples were kept in moulds at 20±1°C and 100% r.h. After 24 hours of formation, the samples were transferred to deionised water and stored there for 27 days at 20 ± 1°C. The hydration of samples was stopped using acetone: at first, samples were crushed, ground by a laboratory vibrating disc mill, washed with acetone and dried at 60 ± 5°C for 6 hours.

The required energy consumption of micro-filler preparation has been estimated using a vibrating disc mill Fritsch Pulverisette 9 at 800 rpm. The study was carried out in two ways: first, raw materials were ground within the same duration and a specific surface area was measured; second, the grinding times were estimated to reach the same specific surface area. Before grinding, all the specimens were crushed with a laboratory jaw crusher (uniform distance between the jaws – 0.5 cm). For the specific surface area measurements,

automatic Blaine apparatus was used.

The XRD analysis was performed on the D8 Advance diffractometer (Bruker AXS, Karlsruhe, Germany) operating at the tube voltage of 40 kV and tube current of 40 mA. The X-ray beam was filtered with Ni 0.02 mm filter to select the CuKα wavelength. Diffraction patterns were recorded in a Bragg-Brentano geometry using a fast counting detector Bruker LynxEye based on silicon strip technology. The specimens of samples were scanned over the range 2θ = 3–70° at a scanning speed of 6° min⁻¹ using a coupled two theta/theta scan type.

Simultaneous thermal analysis (STA: differential scanning calorimetry [DSC] and thermogravimetry [TG]) was carried out on a Netzsch STA 409 PC Luxx instrument with ceramic sample handlers and crucibles of Pt-Rh. At a heating rate of 15 °C/min, the temperature ranged from 30 °C to 1000 °C under the atmospheric pressure.

The calorimetric analysis data were gathered using a TAM AIR III calorimeter. The range of measurement was ±600 mW, the sensitivity of the signal was 4 μW, the time constant was <500 s, the temperature of the experiment was 25 ± 0.1 °C, and the water/solid ratio was 0.5.

Infrared (IR) spectra were measured using a PerkinElmer Fourier transform-IR (FT-IR) system Spectrum X spectrometer. Samples were prepared in a vacuum compressor by mixing 1 mg of the sample in 200 mg of KBr and compressing tablets. The spectral analysis was performed in the range 4000 – 400 cm⁻¹ with a spectral resolution of 1 cm⁻¹. Measurement accuracy ± 0.01 cm⁻¹. The distribution of particle size, specific surface area and particle image of used materials were determined by a laser particle-size-analyzer CILAS 1090 LD 0.04–500 μm interval. The distribution of solid particles in the air stream was 12–15 % wt. Compressed air (2500 mbar) was used as a dispersing phase. Measuring time was 15 s.

Pore structure was investigated using Micromeritics AutoPore III 9400 model mercury intrusion porosimetry (MIP) equipment. Applying pressures range between 0 and 414 MPa (60,000 psi) in two pressure units as low (345 kPa) and high (up to 414 MPa) pressure, respectively. In this study, mercury contact angle and mercury surface tension are taken as 130° and 485 dynes/cm, respectively. The accuracy of total porosity measurements was ± 1%.

3. Results and Discussion

3.1. Properties of AACW

Mineral composition of AACW was determined by the XRD analysis. Figure 1 shows: tobermorite (*d* – 1,132; 0,565; 0,544 nm; JCPDS 19-1364), calcium silicate hydrate C-S-H(I) (*d* –

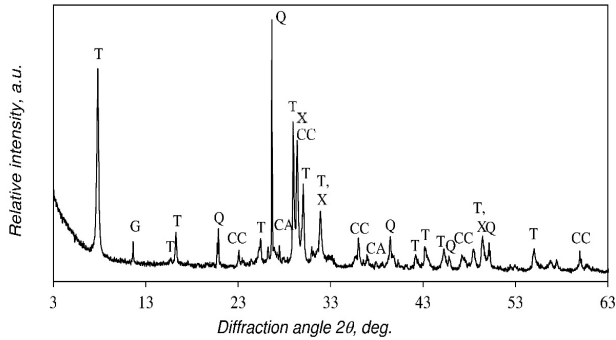


Fig. 1 - X-ray diffraction pattern of AACW sample. Indexes: T – $\text{Ca}_5\text{Si}_6\text{O}_{16}(\text{OH})_2 \cdot 4\text{H}_2\text{O}$ (tobermorite), X – C-S-H(I), CA – C_3AH_6 , CC – CaCO_3 (calcite), G – $\text{CaSO}_4 \cdot 2\text{H}_2\text{O}$ (gypsum), Q – SiO_2 (quartz).

0,303; 0,283; 0,180 nm; JCPDS 3-548), C_3AH_6 (d – 0.514; 0.230; 0.204 nm), calcite (d – 0.302; 0.228; 0.209; 0.189; 0.186 nm; JCPDS 72-1650), quartz (d – 0.425; 0.334; 0.245; 0.181; 0.154 nm; JCPDS 46-1045) and gypsum (d – 0,761; 0,426; JCPDS 3-44) were found in prepared AACW samples.

In DSC curve of AACW sample (Fig. 2, curve 1), the endothermic effect at 100–200 °C can be attributed to the dehydration of calcium silicate hydrate and gypsum, the endothermic effect at 330–340 °C shows the dehydration of calcium aluminium hydrate (C_3AH_6), while at 760 °C – the decomposition of calcite. The exothermic effect at 850 °C shows C-S-H (I) recrystallisation into wollastonite [10, 11].

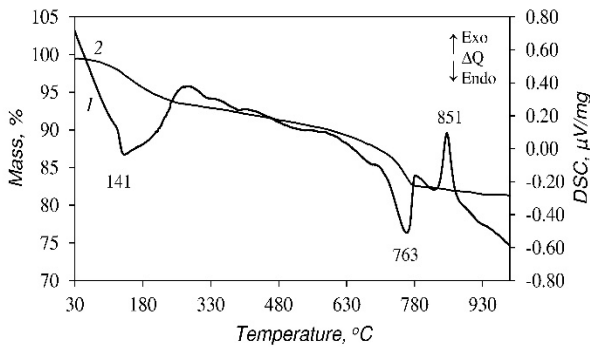


Fig. 2 - Simultaneous thermal analysis (1 – DSC, 2 – TG) curves of AACW

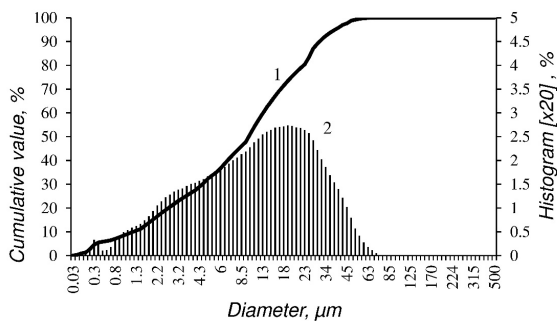


Fig. 3 - Particle size distribution of prepared AACW

The particle size distribution of AACW is shown in Figure 3. It was found that the largest particle diameter reaches 70 µm, and the uniformly distributed particles are dominated with a diameter from 10 to 35 µm. While particles with diameters lesser than 63 µm, represented 95 % wt. of the total amount, according to EN 12620 standard, prepared AACW can be used as a micro-filler (filler aggregate) in cement products.

It is widely known that construction and demolition waste (C&DW) can be used not only as a coarse and/or fine aggregate in concrete production, but also as ultra-fine (filler) material in the construction industry [9]. In cementitious systems finely ground natural rock such as limestone can be also used as a micro-filler. Therefore, in the next stage of the research, the energy consumption, required to prepare micro-filler from different raw materials, namely, AACW, C&DW and limestone, was determined. The results of this investigation are listed in Table 2.

Table 2

Grinding parameters of different raw materials			
Grinding parameters	Raw materials		
	AACW	C&DW	Limestone
Grinding 45 s at	Specific surface area, m ² /kg		
800 rpm	450	110	310
Specific surface area –	Grinding time, s		
450 m ² /kg	45	210	70

The measured specific surface area of C&DW was 4 times and of limestone - 1.5 times lesser to compare with AACW after the same duration of grinding (Table 2). The same trend was observed of measured grinding duration to achieve the same specific surface area (450 m²/kg). According to the results, AACW is much easier to grind and this can be explained by the fact that fine ground sands are used for the production of AAC.

Summarising the results, it can be stated that recycling AAC waste as the micro-filler requires one and a half lesser energy than natural additive limestone and four times lesser energy than ordinary construction and demolition waste.

3.2. Influence of AACW additive on the hydration of Portland cement

In order to assess the influence of AACW additive on the initial hydration of cement, measurement of heat evolution during the hydration process (calorimetric analysis) was performed (Fig. 4). Two intense peaks of heat evolution were found on the calorimetric curves of the investigated samples. The first, an active heat evolution, is caused by wetting cement powder

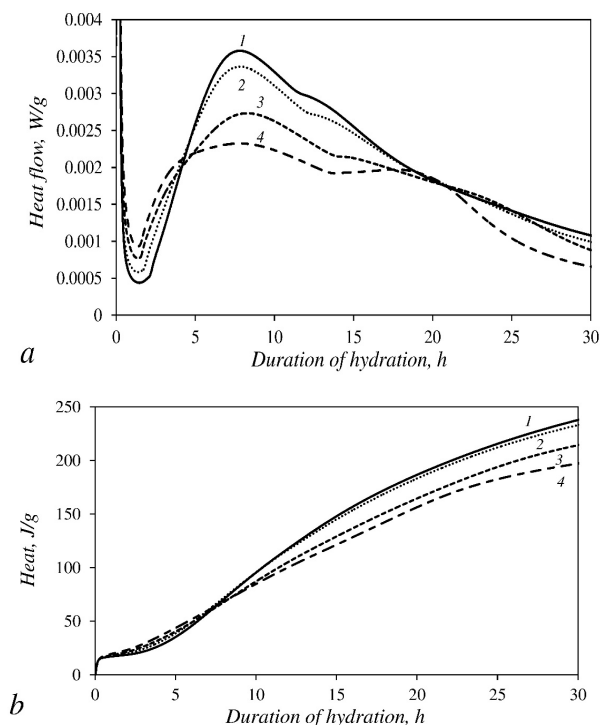


Fig. 4 - Calorimetric curves of thermal flow (a) and heat (b) in samples with different amounts of AACW additive: 1 – Portland cement; 2 – Portland cement with 5 % wt. AACW; 3 – Portland cement with 10 % wt. AACW; 4 – Portland cement with 15 % wt. AACW .

and an initial kinetic reaction, during which Ca^{2+} , OH^- , SiO_4^{4-} , and SO_4^{2-} ions passed into the solution, and the second is related to the reaction between the deeper layers of calcium silicate particles and water [12, 13].

It was determined that the AACW additive significantly shortened the duration of the induction period. Compared with the analysis results of Portland cement samples (1 h 21 min), the induction period was reduced to 1 h 05 min or to 45 min when 5 or 15 % wt. of cement was replaced by AACW, respectively. During the hydration of cement samples with AACW additive, at the second exothermic reaction period, a slightly earlier heat flow than in the Portland cement sample was identified on the released heat flow measurement curve (Fig. 4, a). The maximum heat flow value was reached after 7 h 50 min of hydration in the sample with 5 % wt. additive, 7 h 37 min – in the sample with 15 wt.% additive, whereas in the Portland cement sample it was reached after 7 h 55 min. Therefore, it can be assumed that the AACW additive accelerated the initial Portland cement hydration. It is possible that, during the induction period, Ca^{2+} ions were adsorbed on the surface of the AACW or finely ground additive can act as crystallisation centers, around which portlandite and calcium silicate hydrate begin to crystallise. In both cases, the Ca^{2+} concentration was reduced in the solution, and because of this, the cement hydration was accelerated [14].

The more heat of hydration was identified in samples with AACW additive during the first four hours of hydration. However, after this period, the heat of hydration proportionally decreases with increasing of AACW amount in the cement samples (Fig. 4, b). The induced heat was slightly smaller for samples with 5 % wt. AACW (314 J/g) than of pure cement (319 J/g), while only 256 J/g – for samples with 15 % wt. AACW after 72 h of hydration. Heat evaluation proves that AACW has no binding properties and it plays a significant role as an inert micro-filler, dilutes the cement content in the paste and reduces the total amount of hydration heat.

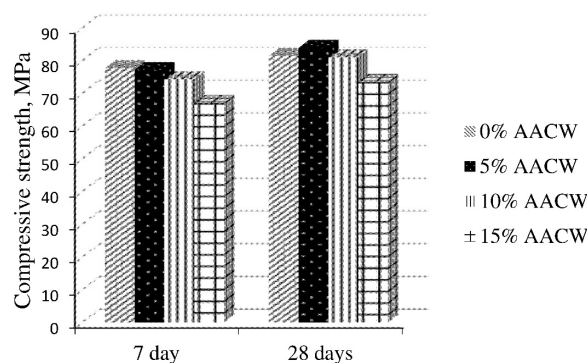


Fig. 5 - Compressive strength of cement samples with different amounts of AACW additive after 7 and 28 days of hydration under normal conditions.

After 7 days of hydration (Fig. 5), the highest, and approximately the same compressive strength was identified for Portland cement paste samples and for samples with 5 % wt. AACW additive. The lower compressive strength was identified for samples with 10 and 15 % wt. AACW additive.

For samples cured 28 days under normal conditions the highest compressive strength was determined for samples with 5 % wt. AACW additive, while for 10 % wt. AACW – the strength was the same as for Portland cement paste (Fig. 5). It is important to note that compressive strength of samples with 15 % wt. AACW showed the weakest values, so it can be stated that 10 % wt. is the highest admissible amount of AACW additive for cement without impairing strength properties of samples. The positive impact of AACW additive on strength properties could be explained by the acceleration of calcium silicate hydration and densification of cement stone.

The best way of densification evaluation can be done by measuring the distribution and the volume of cement stone pores. The investigation of porosity clearly shows (Fig. 6) that cement stone structure with AACW additive is denser, comparing with cement stone of pure Portland cement. After 28 days of hydration under normal conditions, AACW additive decreased the threshold pore diameter, a threshold pore diameter of 0.019 μm

was identified for Portland cement sample, whereas that of sample with 10 % wt. AACW additive was 0.012 μm (Fig. 6). Moreover, compared with the control samples of Portland cement, the total porosity of sample with 10 % wt. AACW additive decreased from 22.72% to 21.48%.

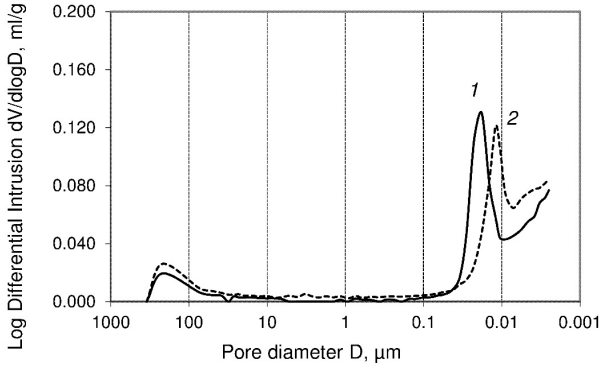


Fig. 6 - Mercury porosimetry log differential intrusion curve patterns of ordinary Portland cement (OPC) (1) and OPC with 10 % wt. AACW additive (2) samples cured for 28 days in water.

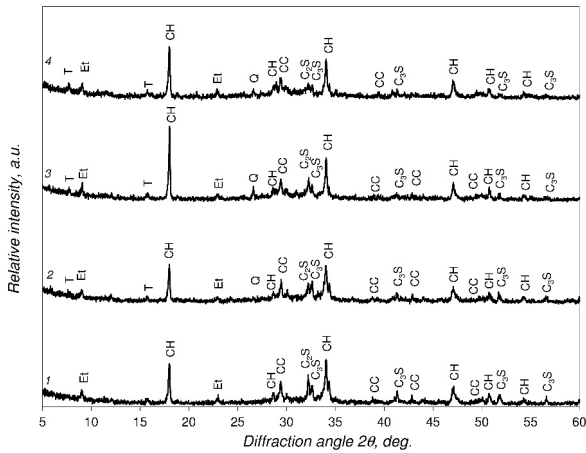


Fig. 7 - X-ray patterns of samples cured for 28 days under normal conditions: 1 – Portland cement; 2 – Portland cement with 5 % wt. AACW; 3 – Portland cement with 10 % wt. AACW; 4 – Portland cement with 15 % wt. AACW. Indexes: CH – $\text{Ca}(\text{OH})_2$ (portlandite), CC – CaCO_3 (calcite), C_3S – Ca_3SiO_5 (tricalcium silicate), C_2S – Ca_2SiO_4 (dicalcium silicate), Et – $(\text{CaO})_3(\text{Al}_2\text{O}_3)(\text{CaSO}_4)_3 \cdot 32\text{H}_2\text{O}$ (ettringite), Q – SiO_2 (quartz), T – tobermorite.

XRD analysis of all paste samples hydrated in water for 28 days (Fig. 7) indicated high-intensity peaks characteristic to portlandite ($d = 0.493$; 0.263 ; 0.193 nm; JCPDS – 1-1079), calcite ($d = 0.304$; 0.192 ; 0.228 ; 0.187 nm; JCPDS – 1-837), unhydrated C_3S ($d = 0.275$; 0.261 ; 0.218 , 0.176 nm; JCPDS – 1-1024), unhydrated C_2S ($d = 0.277$; 0.219 ; 0.262 ; 0.198 nm; JCPDS – 1-1012) and ettringite ($d = 0.980$; 0.279 ; 0.570 ; 0.387 nm; JCPDS – 2-59).

In samples with AACW additive, peaks characteristics to quartz ($d = 0.335$; 0.425 ; 0.182

nm; JCPDS – 1-649) and tobermorite ($d = 1,132$ nm; JCPDS 19-1364) were also identified (the main components of AACW). No changes of diffraction peak intensity characteristic to tobermorite were identified. This data shows that tobermorite from AACW does not react with Portland cement hydrates. This is confirmed by the fact that no other Portland cement hydrates in samples with an AACW additive were identified by XRD analysis. It should be noted that the intensity of unhydrated C_3S and C_2S peaks decrease with an increasing amount of AACW additive from 5 to 15 % wt. in all samples. The lower intensity of unhydrated C_3S and C_2S diffraction peaks may be associated with decreasing of OPC amount in the samples and with more intense hydration process of calcium silicates.

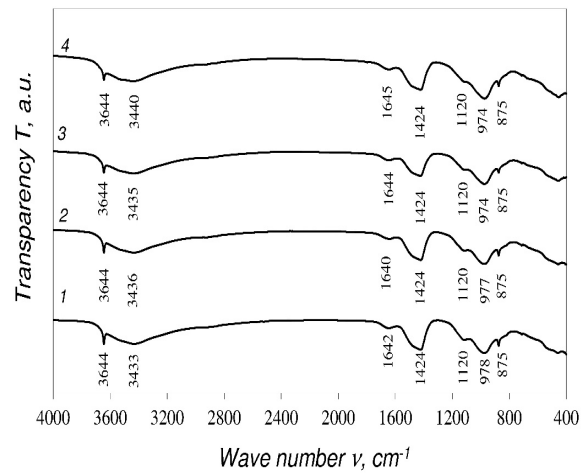


Fig. 8 - Fourier transform–infrared (FT-IR) spectrum of samples cured for 28 days under normal conditions: 1 – Portland cement; 2 – Portland cement with 5 % wt. AACW; 3 – Portland cement with 10 % wt. AACW; 4 – Portland cement with 15 % wt. AACW.

The IR spectrum curves (Fig. 8) of all samples cured for 28 days under normal conditions show absorption bands characteristics for Portlandite (3644 cm^{-1}), calcium carbonate (vibration of CO_3^{2-} at 875 and 1424 cm^{-1}), calcium silicate hydrates ($\nu_3(\text{Si}-\text{O})$ at $974\text{--}978 \text{ cm}^{-1}$) and ettringite (SO_4^{2-} at 1120 cm^{-1}) [15]. The IR spectrum curves and intensity of absorption bands of all samples were closely similar and this (together with XRD analysis data) reasserts that during the hydration process no new compounds were formed in samples with an AACW additive. It is important to note because some authors state [7] that the presence of sulfate in the composition of AACW leads to durability problems.

In all DSC curves of 28 days under normal conditions hydrated samples (Fig. 9), the endothermic effects at $100 \text{ }^\circ\text{C}\text{--}200 \text{ }^\circ\text{C}$ and at $430 \text{ }^\circ\text{C}\text{--}450 \text{ }^\circ\text{C}$ were identified. The endothermic peak at $100 \text{ }^\circ\text{C}\text{--}200 \text{ }^\circ\text{C}$ is due to the dehydration of most cement hydration products (calcium

Table 3

Thermogravimetry analysis results of samples cured for 7 and 28 days under normal conditions

Amount of AACW additive, wt. %	Mass loss, wt. %			
	Temperature range, °C			
	100–200		430–450	
	7 day	28 days	7 day	28 days
0	4.90	5.10	3.23	3.34
5	5.24/4.87*	5.50/5.13*	3.12	3.28
10	5.19/4.81*	5.94/5.56*	3.10	3.26
15	5.31/4.75*	5.61/5.05*	3.09	3.20

* Mass loss without mass loss of AACW (calculated)

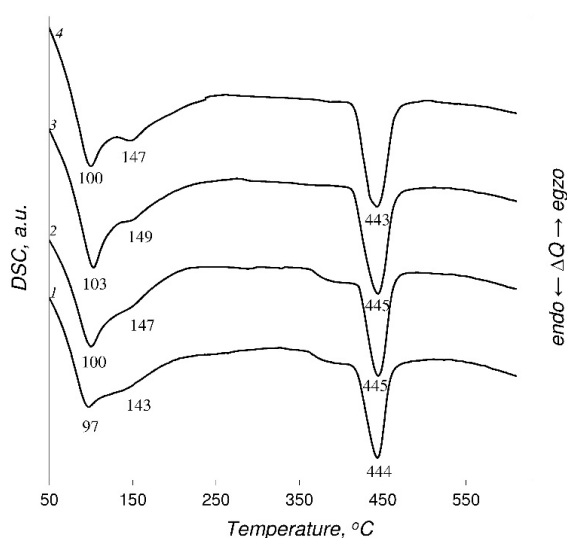


Fig. 9 - Differential scanning calorimetry patterns of samples cured for 28 days under normal conditions: 1 – Portland cement; 2 – Portland cement with 5 % wt. AACW; 3 – Portland cement with 10 % wt. AACW; 4 – Portland cement with 15 % wt. AACW.

silicate hydrates, calcium aluminates, ettringite, etc.), whereas those at 430 °C–450 °C indicate the decomposition of Portlandite [16, 17]. The results of TG analysis are listed in Table 3. Mass loss at the 100 °C–200 °C temperature range was divided into two values: the total mass loss and the mass loss with an excluded effect of evaluated decomposition of AACW additive. (Calculated from TG data, Fig. 2, taking into account that the mass loss of AACW sample at 100–200 °C was 3.8 % wt.:

$$\Delta \text{ mass loss of hydration products} = \Delta \text{ total mass loss} - \Delta \text{ mass loss of additive} \times \% \text{ wt. of additive}.$$

From TG analysis results it can be seen that with an increasing amount of AACW additive, the mass loss due to Portlandite (430 °C–450 °C) dehydration decreases both after 7 and 28 days of hydration. Another trend is visible in the area of other cement hydration products dehydration (100 °C–200 °C). The higher mass loss after 7 days of hydration is observed for Portland cement sample and in the sample with 5 % wt. of AACW additive. However, after 28 days of hydration, the maximum mass loss was observed for the sample with 10 % wt. of AACW additive. The mass loss of sample with 5 % wt. of additive was also greater than for

wt. of AACW additive. The mass loss of the sample with 5 % wt. of additive was also greater than the loss of the Portland cement sample. This tendency remained the same when the mass loss of the AACW additive was excluded (Table 3, marked *), therefore the higher mass loss at 100–200 °C in the samples with 5–10 % wt. of AACW additive is related to the formation of additional amount of calcium silicate hydrates.

Thus, thermal analysis results confirm that AACW promotes the hydration of calcium silicates and formation of the additional amount of calcium silicate hydrates which increases the compressive strength of samples.

4. Conclusions

1. It was estimated that Autoclaved Aerated Concrete Waste consists mainly from quartz and calcium silicate hydrates and recycling of this waste as micro-filler required one and a half less energy than natural additive i.e. limestone and four times less energy than conventional construction and demolition waste use.
2. Under normal conditions, AACW additive shortened the duration of the induction period of ordinary Portland cement hydration and promoted the hydration of calcium silicates.
3. AACW additive does not change the qualitative composition of the cement hydrates but makes the cement stone denser, promotes the formation of an additional amount of calcium silicate hydrates, and, therefore, up to 10 % wt. of ordinary Portland cement can be replaced by AACW additive without impairing the strength properties of samples.

REFERENCES

1. A. Korpa, T. Kowald, R. Trettin, Hydration behavior, structure and morphology of hydration phases in advanced cement-based systems containing micro and nanoscale pozzolanic additives. *Cem. Concr. Res.*, 2008, **38**(7), 955.
2. C. Jaturapitakkul, J. Tangpagasit, S. Songmue, K. Kiattikomol, Filler effect and pozzolanic reaction of ground palm oil fuel ash. *Constr. Build. Mat.*, 2011, **25**(11), 4287.
3. G. Isaia, A. Gastaldini, R. Moraes, Physical and pozzolanic action of mineral additions on the mechanical strength of high-performance concrete. *Cem. Concr. Comp.*, 2003, **25**(1), 69.
4. W. Jackiewicz-Reka, K. Załęgowska, A. Garbacza, B. Bissonnetteb, Properties of cement mortars modified with ceramic waste fillers. *Proc. Engineer.*, 2015, **108**, 681.

5. L. Courard, F. Michel, Limestone fillers cement based composites: Effects of blast furnace slags. *Constr. Build. Mat.*, 2014, **51**, 439.
6. A. Goldman, A. Bentur, The influence of microfillers on enhancement of concrete strength. *Cem. Concr. Res.*, 1993, **23** (4), 962.
7. J. Bergmans, P. Nielsen, K. Broos, R. Snellings, M. Quaghebeur, Recycling of autoclaved aerated concrete in screed and stabilized sand. Conference Paper, 2015, DOI: 10.5281/zenodo.46405
8. W. Arayaprane, G. L. Rempel, Autoclaved aerated concrete waste (AACW): An alternative filler material for the natural rubber industry. *Polym. Comp.*, 2015, **36** (11), 2030.
9. T. Yılmaz, B. Ercikdi, H. Deveci, Utilisation of construction and demolition waste as cemented paste backfill material for underground mine openings. *J. Environ Manage.*, 2018, **222**, 250.
10. D. Niuniavaite, K. Baltakys, T. Dambrauskas, The Adsorption Kinetic Parameters of Co^{2+} Ions by $\alpha\text{-C}_2\text{SH}$. *Buildings*, 2018, **8**, 10.
11. K. Baltakys, T. Dambrauskas, R. Siauciunas and A. Eisinias, The formation of $\alpha\text{-C}_2\text{S}$ hydrate in the mixtures with $\text{CaO/SiO}_2 = 1.75$ by hydrothermal treatment at 200 °C, *Romanian Journal of Materials*, 2014, **44** (1), 109.
12. B.,W. Langan, K. Weng, M.A. Ward, Effect of silica fume and fly ash on heat of hydration of Portland Cement. *Cem. Concr. Res.*, 2002, **32** (7), 1045.
13. D. G. Snelson, S. Wild, M. O'Farrell, Heat of hydration of Portland Cement-Metakaolin-Fly ash, (PC-MK-PFA) blends. *Cem. Concr. Res.*, 2008, **38**(6), 832.
14. P.K. Mehta, Studies on the mechanisms by which condensed silica fume improves the properties of concrete: durability aspects. International Workshop on Condensed Silica Fume in Concrete, 1987, 1.
15. X.Wang, Z. Pan, X. Shen, W. Liu, Stability and decomposition mechanism of ettringite in presence of ammonium sulfate solution. *Constr. Build. Mat.*, 2016, **124**, 786.
16. W. Sha, E.A. O'Neill, Z. Guo, Differential scanning calorimetry study of ordinary Portland cement. *Cem. Concr. Res.*, 1999, **29** (9), 1487.
17. M.M. Radwan, M. Heikal, Hydration characteristics of tricalcium aluminate phase in mixes containing β -hemihydrate and phosphogypsum. *Cem. Concr. Res.*, 2005, **35** (8), 1601.

MANIFESTĂRI ȘTIINȚIFICE / SCIENTIFIC EVENTS

2nd International Conference on Sustainable Building Materials 12 – 15.08, Eindhoven University of Technology, The Netherlands

Main topics:

New cementitious binders: engineered OPCs, supplementary cementitious binders, alkali-activated binders, calcium sulfoaluminate cement (CSA), magnesium oxychloride cement (MOC), calcined clays, etc.
Hydration, modelling, performance, durability, and repair.

Greened materials/products: concrete, autoclaved aerated concrete, woodwool cement composites, gypsum wallboards, fired clay, unconventional clays and aggregates, alternative chemical admixtures, mortars, etc.

Waste recovery, treatments and valorisation: municipal solid waste incineration residues, steel converter slags, mine tailings, paper sludge incineration ashes, biomass incineration ashes, etc.
Characterization of waste residues, enhancing treatments (physical, chemical and thermal), alternative raw materials, second life, environmental impact, modelling of hydration and leaching etc.

Biogenic materials: bio-fibers, bio-aggregates, alternative natural fibers, agricultural and biorefinery residues etc.

Functionalized materials: nano-engineered, coated, photocatalytic, self-cleaning, self-healing, hydrophobic, etc.

Contact: https://susbuildmat.com/?page_id=52
